Enhancing Measured MIMO Capacity by Adapting the Locations of the Antenna Elements

by

Jeng-Shiann Jiang and Mary Ann Ingram

{jsjiang@ece.gatech.edu, mai@ece.gatech.edu}

School of Electrical and Computer Engineering
Georgia Institute of Technology

ENHANCING MEASURED MIMO CAPACITY BY ADAPTING THE LOCATIONS OF THE ANTENNA ELEMENTS

Jeng-Shiann Jiang and Mary Ann Ingram

School of Electrical and Computer Engineering, Georgia Institute of Technology, Atlanta, GA 30332-0250, USA
gte345k@prism.gatech.edu and mai@ece.gatech.edu

Abstract – We show that the multiple-input, multiple-output (MIMO) capacity of measured, indoor flat-fading channels may be improved by adaptively changing the locations of the antenna elements. Moving the antenna elements is a way to provide spatial diversity to a MIMO link without decreasing the number of parallel data streams. First, we demonstrate that significant variations in equal-power capacity are possible using measured data from finely sampled virtual arrays at both ends of a MIMO link. Second, using steepest descent and a simulated path-type channel derived from measured data, we adapt the element locations. In line-of-sight (LOS) and obstructed-line-of-sight (OLOS) examples, the local maximum capacity is reached within 5 and 10 iterations, respectively. The improvements relative to the equally spaced arrays are approximately 22% and 19%, respectively.

Keywords – MIMO, adaptive array, array signal processing.

I. INTRODUCTION

Multiple-input multiple-output (MIMO) or spatially multiplexed wireless links have received a great deal of recent attention because they can provide extremely high spectral efficiencies in rich multipath environments [1]. Usually, the studies of these links assume that the matrix of complex channel gains between all possible transmit-receive antenna pairs is given, and the object of the study is how to best determine the excitations of the transmit antenna elements and the combining methods used at the receive array [2-5]. Many of these studies are concerned with the Shannon capacity of the flat-fading MIMO link and most are based on simulated channels [3-4]. A couple of research groups have not made the "given channel" assumption. One group has considered theoretically how optimization of the antenna element locations at both ends of a normalized link might affect the distribution of singular values of the channel matrix for the best and worst cases of Shannon capacity [9-10]. The other group has found significant SNR improvements for spatial multiplexing over simulated channels by adaptively selecting only a subset of the available transmit antennas [6-8]. This latter work may be thought of as an adaptive element location approach, where the adaptation is only at one end of the link, and the locations are very coarsely quantized. In this paper, we consider adapting the locations of elements at both ends of the link. We use virtual or synthetic arrays at both ends of the link to determine how the equal-power capacity varies for small changes in element locations.

This paper is organized as follows. Section II provides the description of our MIMO channel measurement system and the experiment environment. In Section III, we present the Shannon capacity of a real MIMO indoor channel at 5.8 GHz as a function of finely quantized element locations, and we compare these results to an ensemble of measured capacities for equally spaced arrays as well as for the ideal iid MIMO channel. We demonstrate that significant enhancement of the capacity is possible by adapting the element locations. Section IV provides a brief description of the path-parameter estimation technique and presents the results of simulations of the adaptive array.

II. THE MIMO CHANNEL MEASUREMENT SYSTEM

As illustrated in Figure 1, our MIMO-channel measurement system is composed of two parts: (1) the HP 85301B stepped-frequency antenna pattern measurement system, which, because of its coherent reference signal, can measure the channel frequency response directly, and (2) the actuator positioning system, which creates the virtual array by moving the antenna to arbitrary pre-programmed locations. Figure 2 shows one of the mobile platforms and one of the actuator positioning systems. There were two of the setups shown in Figure 2, one for each end of the MIMO channel.

The antennas used at both sites were omni-directional, vertically polarized, wideband biconical antennas with frequency range 2.5 – 18 GHz. For the measurements reported in this paper, the transmitted signals were centered at 5.8 GHz with a power of 20 dBm. The noise floor was –120 dBm. In the virtual array approach, the environment must be kept still while the measurements are being taken. In order to achieve this, all the experiments were conducted after midnight. Repeatability was verified by taking 60 identical measurements in about one hour. The experiments show that the average variance-to-signal-ratio (VSR) is around -30 to - 40 dB.

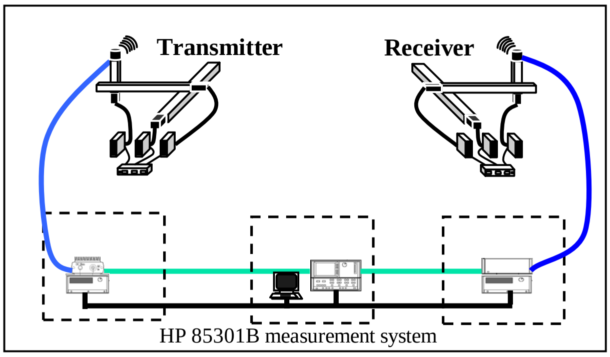

Figure 1. MIMO channel measurement system.

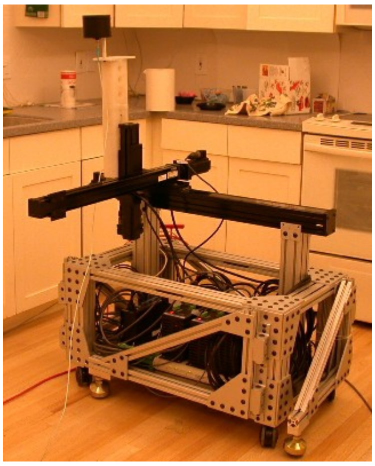

Figure 2. 3D actuator system on mobile platform.

III. THE POTENTIAL OF THE ADAPTIVE ARRAY

A. Measurement procedure

To investigate how the channel capacity changes with the array geometry, and how much benefit we can get by the adaptive array, we conducted an experiment to measure the channel matrix of arrays with finely separated elements. We made the measurements in the Smart Antenna Laboratory of the Georgia Center of Advanced Telecommunication Technology (GCATT) Building. The Tx and the Rx arrays were placed in separate rooms. There was an open door joining the rooms, but no line-of-sight (LOS) path was available in the MIMO channel. In the first experiment, the transmitted signal was a single tone of 5.8 GHz with the power of 20 dBm. At both the Tx and Rx, we synthesized 61-element uniform linear arrays (ULAs), with the sample spacing of 0.1 λ where λ is the wavelength of the 5.8 GHz signal. We note that a virtual array has no mutual coupling, regardless of the sample spacing. The channel matrices of a large number of unequally spaced arrays can be determined as subsets of the measured (61,61) MIMO channel.

B. MIMO capacity with varying element locations

First, we investigate the capacity of the (4,4) MIMO link with an unequally spaced array. The antenna locations of the Tx and Rx arrays are denoted as $\mathbf{x}_T = (x_{T1}, x_{T2}, x_{T3}, x_{T4})$ and $\mathbf{x}_R = (x_{R1}, x_{R2}, x_{R3}, x_{R4})$, respectively. To simplify the situation, at first we use the fixed uniform array at the Tx site, and allow only the second and third antennas of the Rx array to be changed. Therefore, the antenna locations of both arrays are

$$\begin{aligned} \mathbf{x}_T &= (x_{T1}, x_{T2}, x_{T3}, x_{T4}) = (0, 2\lambda, 4\lambda, 6\lambda) \\ \mathbf{x}_R &= (x_{R1}, x_{R2}, x_{R3}, x_{R4}) = (0, x_{R2}, x_{R3}, 6\lambda), \\ \text{where } & x_{R2} \in \{ n \times 0.1\lambda \mid 2 \le n \le 59 \} \\ & x_{R3} \in \{ n \times 0.1\lambda \mid 3 \le n \le 60 \} \end{aligned} \quad (1)$$

Later, the second and third elements of the Tx array are allowed to vary in addition to the two Rx elements. For each set of the element positions, the equal-power MIMO capacity is calculated [1] as

$$C = \log_2 \det \left[I_{N_R} + (SNR / N_T) \cdot HH^{\dagger} \right]. \quad (2)$$

Figure 3 shows the measured capacities of the MIMO system with varying x_{R_2} and x_{R_3} when SNR is 30 dB and for one pair of locations of the array measurement platforms.

According to the results, the capacity is 34.04 (bits/sec/Hz) for the single MIMO channel when the Rx array is uniform. The maximum capacity of 38.29 (bits/sec/Hz) is achieved when $\mathbf{x}_R = (0, 1.1\lambda, 5.3\lambda, 6\lambda)$, while the minimum capacity of 28.59 (bits/sec/Hz) occurred when $\mathbf{x}_R = (0, 0.6\lambda, 2.9\lambda, 6\lambda)$. In Figure 4, the two circle symbols indicate these max and min values. The solid curve is the measured Shannon capacity when both Tx and Rx arrays were uniform. Comparing the upper circle to this curve, we observe a 3 dB SNR improvement from variation of only the two internal Rx array elements. When the second and third antennas in the Tx array are also changeable, the capacity can be further improved. In this case, the maximum capacity is 40.94 (bits/sec/Hz) when $\mathbf{x}_T = (0, 0.8\lambda, 3.3\lambda, 6\lambda)$ and $\mathbf{x}_R = (0, 1.1\lambda, 4.3\lambda, 6\lambda)$.

The extreme capacity values for joint Tx and Rx adaptation are also shown as boxes in Figure 4, where the SNR improvement of 5dB is evident. These critical capacities are summarized and denoted in Table I.

It is of interest to see how the capacities of the arrays with adapted element locations compare to the ensemble of capacities that are possible with a uniform array. To measure the ensemble, we conducted another experiment where the Tx and Rx array platforms were in the same locations as the previous measurement. In this experiment, 6-element uniform linear arrays with antenna spacing 2λ were synthesized at both the Tx and Rx. Accordingly, nine equally spaced (4,4) subarrays can be extracted from the acquired (6,6) channel matrix. In order to increase the number of samples, we repeated the measurements at 51 different frequencies with 2 MHz spacing, centered at 5.8 GHz. Therefore, we obtained 9×51=459 outcomes of the capacity of a (4,4) equally spaced array. Likewise, we also collected several capacity outcomes for (*n*,*n*) subarrays

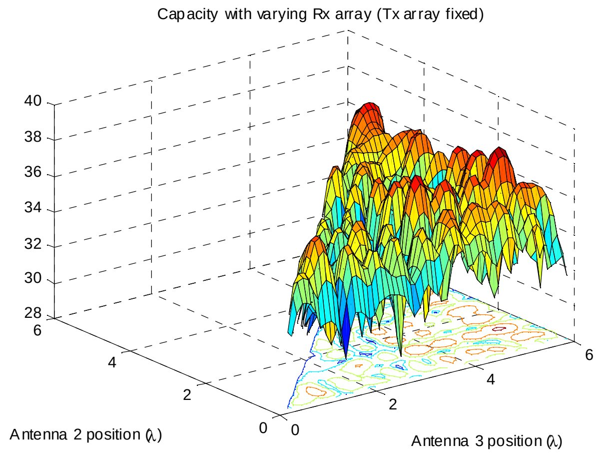

Figure 3. MIMO capacity with varying spacing in Rx array.

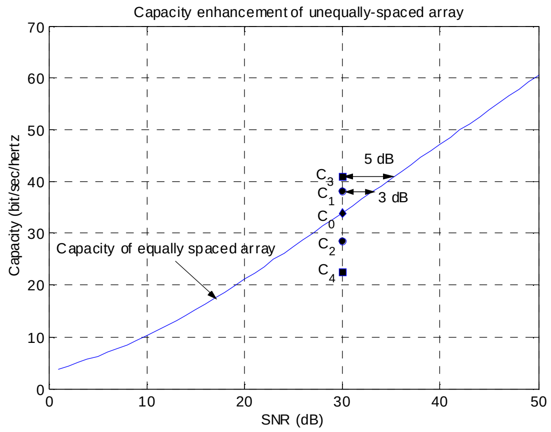

Figure 4. MIMO capacities of the best and worst cases of the adaptively spaced Rx array (circles) and the best and worst cases of the jointly adapted Tx and Rx arrays (boxes). The solid curve is for uniform arrays at both ends.

Table 1. MIMO capacity of various configurations

	Capacity (bit/sec/Hz)	Description
C_0	34.04	equally spaced array
C_1	38.29	max. capacity by moving Rx
C_2	28.59	min. capacity by moving Rx
C_3	40.94	max. capacity by moving Tx and Rx
C_4	22.61	min. capacity by moving Tx and Rx

where $2 \le n \le 6$. Figure 5 depicts the MIMO capacity CDFs of the subarrays with various sizes. This measured data confirms the theory that the MIMO capacity should increase linearly with the number of antennas. The capacities of the arrays with adapted element locations from Figure 4 are included as symbols in Figure 5.

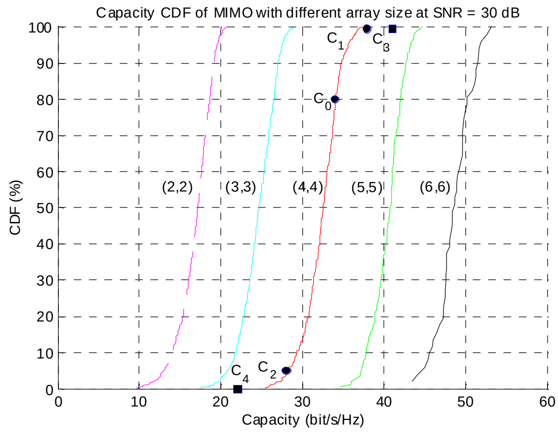

Figure 5. Comparison of unequally and equally spaced MIMO system.

In the experiment, the (4,4) equally spaced MIMO system has an average capacity of 32.36 (bits/sec/Hz) with the standard deviation 1.70 (bits/sec/Hz). We observe the C_0 result was at the 80^{th} percentile, and therefore from a favorable channel. This implies that relative to the mean capacity, the SNR improvements corresponding to C_1 and C_3 are better than the 3 dB and 5 dB mentioned previously. Notice that C_1 = 38.29 (bits/sec/Hz) has passed the maximum capacity 37.67 (bits/sec/Hz) of (4,4) equally spaced array, and the maximum capacity C_3 = 40.94 (bits/sec/Hz) of (4,4) unequally spaced array has even exceeded the average capacity 40.5 (bits/sec/Hz) of the (5,5) equally spaced MIMO system.

Even with 2λ element separations, we found some evidence of correlation in fading across antenna elements. This can be

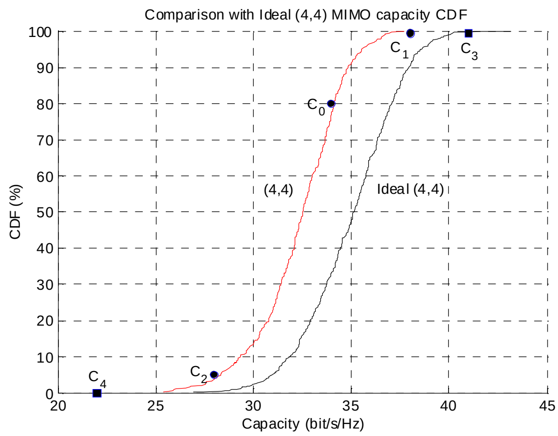

Figure 6. Comparison of unequally spaced MIMO with ideal MIMO channel capacity.

observed In Figure 6 by comparing our measured capacities to those for 2000 trials of an ideal iid complex Gaussian matrix channel with the same average channel gains.

It is interesting to observe that C_3 coincides with the highest capacity of the iid MIMO channel. This means that for the given real multipath environment, enough variation of the channel matrix was induced to reach the extreme outcome by moving just 4 of the total of 8 elements. In other words, this result suggests that, as the subsets of elements are moved in time, the resulting capacity has an ergodic variation.

According to the theory in [9], the maximum capacity for the normalized channel matrix is achieved by making all the eigenvalues equal when the SNR is large. On the other hand, the worst capacity occurs when all eigenvalues are nonzero, equal, and small, except for one which dominates. The measured eigenvalue distributions shown in Table 2 tend to suggest the conclusions of [9].

Table 2. Eigenvalues distributions

Capacity	C_0=34.03	C_1=38.29	C_2=28.59	C_3=40.94	C_4=22.61
Eigen-values	0.0019 0.0009 0.0004 0.0003	0.0015 0.0011 0.0008 0.0006	0.0015 0.0007 0.0005 0.0000	0.0016 0.0013 0.0010 0.0009	0.0016 0.0005 0.0001 0.0000

IV. SIMULATION OF THE ADAPTIVE ARRAY

A. Path- parameter estimation

We next simulated the adaptive algorithm on channel model that was derived from measured data. Similarly to [11], we used multi-dimensional ESPRIT to estimate the number of paths and the loss, delay, direction-of-arrival (DOA) and direction-of-departure (DOD) of each path. However, the ESPRIT algorithm used here differs from that in [11] in that the DOAs (DODs) for the LOS are not assumed to be equal for all Tx (Rx) antenna elements [12]. As an indication of the quality of our path model, we compare in Figure 7 the capacity CDFs for the directly measured channels (following the same procedure as for Figure 5) and the channels reconstructed from the estimated path parameters. Five different antenna spacings are considered.

In Figure 7, the left column corresponds to the directly measured channels and the right column corresponds to the reconstructed channels. Different rows of graphs correspond to different array geometries. In Figure 7(a), the Tx is a 4-element ULA, while the Rx is a 2×2 uniform rectangular array (URA). In Figure 7(c) and (d), both arrays are 4-element ULA, but the Tx is orthogonal to Rx in (c), whereas Tx was parallel with Rx in (e). We observe that the curves on the left closely match the corresponding curves on the right. This indicates that our path model is useful for evaluating MIMO channel capacities.

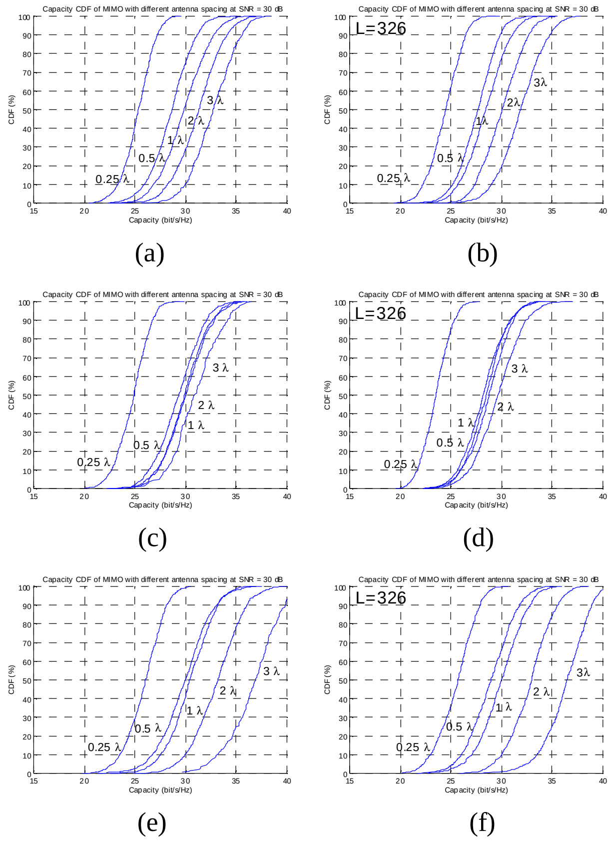

Figure 7. The measured (left) and estimated (right) capacity.

B. Adaptive array with steepest descent algorithm

The implementation of the adaptive array with steepest descent algorithm is shown below.

1. Decide the initial locations of Tx and Rx. In this paper, the Tx and Rx are ULA with antenna spacing = 2λ.
2. Calculate the MIMO channel matrix and its capacity.
3. Move each antenna slightly, e.g., 0.001λ to calculate the capacity gradient.
4. Move the antennas along the direction of gradient. Use quadratic interpolation method [13] to determine the optimum step size.
5. Repeat steps 2-4 until the improvement or step size is less than specified value.

The first experiment has LOS, and the Tx-Rx distance is 2.56 m. As depicted in Figure 8 (a), the capacity achieves 36.8 (bit/sec/Hz) after 3 iterations. Compared to the ULA, the capacity improvement is 21.7%, even though the movements are quite small as we see in Figure 8 (b) (c). For the second experiment, the LOS is obstructed, and the Tx-Rx distance is about 6 m. In Figure 9, we find the capacity changes from 31.34 (bit/sec/Hz) to 37.4 (bit/sec/Hz) after 8 iterations. The improvement is 6.06 (bit/sec/Hz) or 19.3%. The change of the array locations is still small.

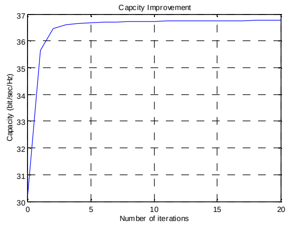

(a) Capacity at each iteration

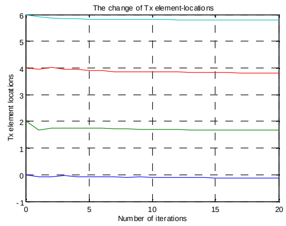

(b) Tx locations

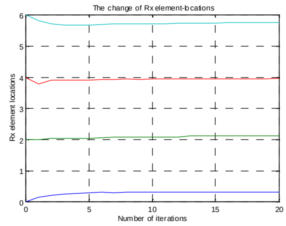

(c) Rx locations

Figure 8. The performance of adaptive array in LOS channel.

(a) Capacity at each iteration

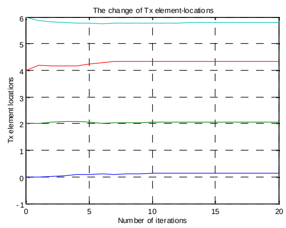

(b) Tx locations

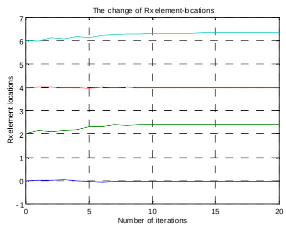

(c) Rx locations

Figure 9. The performance of adaptive array in OLOS channel.

V. CONCLUSION

We have shown that measured MIMO channel capacity changes significantly with slight changes in element locations. Furthermore, simulated element location adaptation using the steepest descent algorithm provided an improvement of the capacity up to 21.7 %, with a small number of iterations. In the future, we will investigate the performance of the adaptive array with more antenna elements, different array shapes, and by adapting the element locations of the virtual arrays over real channels.

REFERENCES

[1] G.J. Foschini and M.J. Gans, “On limits of wireless communications in a fading environment when using multiple antennas,” Wireless Personal Communications, pp.311-335, 1998.

[2] J.H. Winters, J. Salz, znd R.D. Gitlin, “The impact of antenna diversity on the capacity of wireless communication systems,” IEEE Trans. Communications, vol. 42, pp. 1740-1751, Feb. 1994.

[3] G.G. Raleigh and J.M. Cioffi, “Spatio-temporal coding for wireless communication,” IEEE Trans. Communications, vol. 46, pp. 357-366, March 1998.

[4] D. Shiu, G.J., Foschini, M.J. Gans, and J.M. Kahn, “Fading correlation and its effect on the capacity of multielement antenna systems,” IEEE Trans. Communications, vol. 48, pp. 502-513, March 2000.

[5] D. Gesbert, H. Bolcskei, D. Gore, and A. Paulraj, “MIMO wireless channels: capacity and performance prediction,” IEEE GLOBECOM, vol. 2, pp. 1083-1088, 2000.

[6] R.W. Heath, S. Sandhu, and A. Paulraj, “Antenna selection for spatial multiplexing systems with linear receivers,” IEEE Communications Letters, vol. 5, pp. 142-144, April 2001.

[7] S. Sandhu, R.U. Nabar, D.A. Gore, and A. Paulraj, “Near-optimal selection of transmit antennas for a MIMO channel based on Shannon capacity,” IEEE Conference on Signals, Systems, and Computers, vol. 1, pp. 567-571, 2000.

[8] D. Gore and A. Paulraj, “Space-time block coding with optimal antenna selection,” IEEE International Conference on Acoustics, Speech, and Signal Processing, vol. 4, pp. 2441-2444, 2001.

[9] N. Chiurtu and B. Rimoldi, “Varying the antenna locations to optimize the capacity of multi-antenna Gaussian channels,” IEEE International Conference on Acoustics, Speech, and Signal Processing, vol. 5, pp. 3121-3123, 2000.

[10] N. Chiurtu, B. Rimoldi, and E. Telatar, “On the capacity of multi-antenna Gaussian channels,” IEEE International Symposium on Information Theory, pp. 53, June 2001.

[11] J-S, Jiang, M. Ingram, “Path models and MIMO capacity for measured indoor channels at 5.8 GHz,” to be published in International Symposium on Antenna Technology and Applied Electromagnetics, Aug. 2002.

[12] A. Hutter, F. Platbrood, and J. Ayadi, “Analysis of MIMO capacity gains for indoor propagation channels with LOS component,” to be published in IEEE International Symposium on Personal, Indoor and Mobile Radio Communications, Sep. 2002.

[13] J.H. Mathews, “Numerical Methods for Computer Science, Engineering, and Mathematics,” Prentice-Hall, Inc., 1987.